Mechanisms of the Axial Ligand Substitution Reactions of Dinuclear, Head-to-Head α-Pyrrolidonato- and Pivalamidato-Bridged *cis*-Diammineplatinum(III) Complexes with Halide Ions

Kazuhiro Shimazaki,[a] Hideo Sekiya,[a] Haruhiko Inoue,[a] Nami Saeki,[a] Koji Ishihara,*[d] and Kazuko Matsumoto*[e]

Keywords: Platinum / Kinetics / Mechanism / α-Pyrrolidone / Pivalamide

The acid dissociation constant of the axial aqua ligand in the Head-to-Head (HH) dinuclear pivalamidato-bridged *cis*-diammineplatinum(III) complex ($[(H_2O)Pt(NH_3)_2(\mu\text{-}C_5H_{10}NO)_2Pt(NH_3)_2(H_2O)]^{4+}$) and the formation constants of the successive substitution reactions on the axial sites of the HH α-pyrrolidonato-bridged *cis*-diammineplatinum(III) dinuclear complex and the HH pivalamidato-bridged *cis*-diammineplatinum(III) dinuclear complex with halide ions X^- ($X^- = Cl^-$ and Br^-) to give monohalo and dihalo complexes were determined spectrophotometrically at 25 °C and $I = 2.0$ M. A kinetic study was also performed for the monohalo and dihalo complex formations. The effect of the bridging ligand upon the axial site reactivity was compared and discussed. The ligand substitution behavior of the monohalo complex was affected by the axial ligand on the opposite Pt site and also by the bridging ligand. For both the α-pyrrolidonato- and the pivalamidato-bridged complexes, the formation of dichloro complexes proceeds only through the simple substitution path (k_2 path), whereas the formation of dibromo complexes proceeds through the two parallel reaction paths: the k_2 and k_3 paths for the former and the k_2 and $k_2^{\#}$ paths for the latter. The difference of the reaction paths is reasonably explained by the different *trans* effect of the halide ion on the opposite axial site for the former complex, but for the latter complex, the reaction paths are not easy to explain.

Introduction

Head-to-head (HH) amidato-bridged platinum(III) dinuclear complexes containing a metal-metal bond are formed by oxidation of the mixed-valent "platinum blues".[1−11] The two platinum atoms in the dinuclear complexes are nonequivalent: one is coordinated by two ammine nitrogen atoms and two amidate oxygen atoms [$Pt(N_2O_2)$], whereas the other is coordinated by four nitrogen atoms [$Pt(N_4)$], as shown below. The head-to-tail (HT) isomer, in which the two platinum atoms are equivalent, is also known.[4] In our previous reports,[12,13] the kinetics of the axial aqua ligand substitution with halide ions in the HH and HT α-pyridonato-bridged dimers were reported. On both of the HH and HT dimers, the axial ligand substitution occurs in two steps [Equation (1) and (2)].

$$[(H_2O)Pt(NH_3)_2(\mu\text{–}C_5H_4NO)_2Pt(NH_3)_2(H_2O)]^{4+} + X^- \xrightleftharpoons{\text{Step 1}} [(H_2O)Pt(NH_3)_2(\mu\text{–}C_5H_4NO)_2Pt(NH_3)_2(X)]^{3+} + H_2O \quad (1)$$

$$[(H_2O)Pt(NH_3)_2(\mu\text{–}C_5H_4NO)_2Pt(NH_3)_2(X)]^{3+} + X^- \xrightleftharpoons{\text{Step 2}} [(X)Pt(NH_3)_2(\mu\text{–}C_5H_4NO)_2Pt(NH_3)_2(X)]^{2+} + H_2O \quad (2)$$

In the HT dimer, the first halide substitution occurs at one of the two equivalent Pt^{III} atoms, and the first deprotonation occurs at the H_2O of the other Pt^{III} atom; in the HH dimer, the first deprotonation occurs at the H_2O on the $Pt(N_4)$ atom, and the first halide substitution takes place at the $Pt(N_2O_2)$ atom. These phenomena show that the axial halide exerts a *trans* effect through the Pt−Pt bond to the other axial H_2O ligand after the first substitution in both of the HH and HT dimers. In the second halide substitution at the other Pt atom, the substitution lability is influenced strongly by the first halide ligand on the opposite axial site,

---

[a] Department of Chemistry, School of Science and Engineering, Waseda University,
3-4-1 Okubo, Shinjuku-ku, Tokyo 169-8555, Japan
Fax: (internat.) + 81-3/3208-2735
E-mail: ishi3719@waseda.jp
kmatsu@waseda.jp

[b] Materials Research Laboratory for Bioscience and Photonics, Graduate School of Science and Engineering, Waseda University,
3-4-1 Okubo, Shinjuku-ku, Tokyo 169-8555, Japan

[c] Advanced Research Institute for Science and Engineering, Waseda University
3-4-1 Okubo, Shinjuku-ku, Tokyo 169-8555, Japan

Supporting information for this article is available on the WWW under http://www.eurjic.org or from the author.

DOI: 10.1002/ejic.200200565

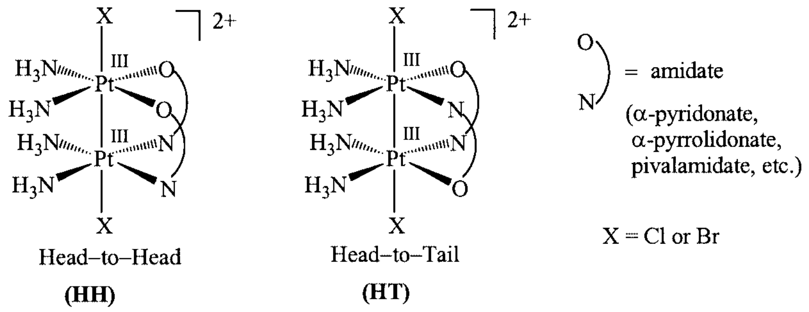

as the charge localization along the Pt−Pt axis is triggered by the first halide ligand, and the extent of the charge localization in the Pt−Pt bond in the dimer {the contribution of HH-$[(X)Pt^{IV}(N_2O_2)\text{-}Pt^{II}(N_4)(H_2O)]^{3+}$ and HT-$[(X)Pt^{IV}(N_3O)\text{-}Pt^{II}(N_3O)(H_2O)]^{3+}$} depends largely on the electron donating ability of the first substituted ligand (X^-).

In this paper we report a kinetic and equilibrium study of the axial aqua ligand substitution with halide ions in the HH α-pyrrolidonato-bridged dinuclear Pt^{III} complex $[(H_2O)Pt(NH_3)_2(\mu\text{-}C_4H_6NO)_2Pt(NH_3)_2(H_2O)]^{4+}$ and the HH pivalamidato-bridged dinuclear Pt^{III} complex $[(H_2O)Pt(NH_3)_2(\mu\text{-}C_5H_{10}NO)_2Pt(NH_3)_2(H_2O)]^{4+}$ (Scheme 1), in order to examine the effect of the bridging ligand on the axial ligand substitution.

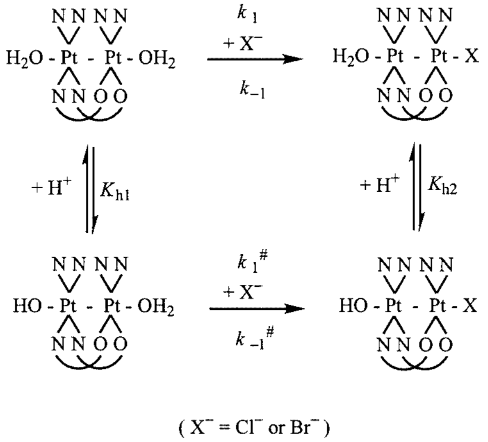

Scheme 1. ($X^- = Cl^-$ or Br^-)

Results

Formation Constants of the HH α-Pyrrolidonato-bridged and the HH Pivalamidato-bridged Monohalo and Dihalo Dimer Complexes

The absorption spectra were measured at $I = 2.00$ M and 25 °C for solutions with various ratios of halide ion concentration, C_{X^-}, ($X^- = Cl^-$ or Br^-) to a fixed dimer concentration, C_{HH}, and are shown in Figure 1 and 2. Several distinct isosbestic points are observed. The spectral changes with varying C_{X^-} are much the same as those for the α-pyridonato-bridged dimers reported previously.[12,13] Therefore, this spectral change corresponds to the following stepwise reactions [Equation (3) and (4)], i.e., the first substitution occurs at the $Pt(N_2O_2)$ atom and the second at the $Pt(N_4)$ atom.

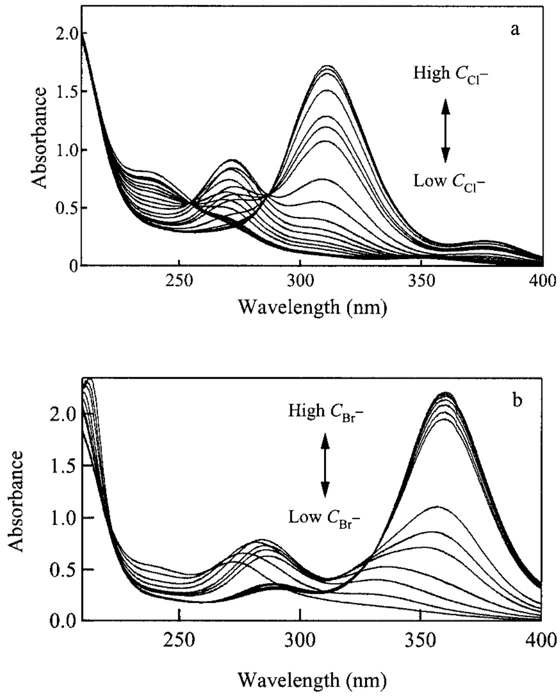

Figure 1. The UV/Vis spectra of the HH α-pyrrolidonato-bridged dimer in acidic aqueous solution with different C_{X^-} at 25 °C and $I = 2.0$ M. $[H^+] = 1.27$ M (a); $[H^+] = 0.401$ M (b), $C_{Cl^-} = 0-4.1 \times 10^{-3}$ M (a); $C_{Br^-} = 0-2.1 \times 10^{-3}$ M (b); $C_{HH} = 9.6 \times 10^{-5}$ M (a), $C_{HH} = 3.9 \times 10^{-5}$ M (b)

$$[H_2O\text{–}Pt(N_4)\text{–}Pt(N_2O_2)\text{–}H_2O]^{4+} + X^- \xrightleftharpoons{K_1^X} [H_2O\text{–}Pt(N_4)\text{–}Pt(N_2O_2)\text{–}X]^{3+} + H_2O \quad (3)$$

$$[H_2O\text{–}Pt(N_4)\text{–}Pt(N_2O_2)\text{–}X]^{3+} + X^- \xrightleftharpoons{K_2^X} [X\text{–}Pt(N_4)\text{–}Pt(N_2O_2)\text{–}X]^{2+} + H_2O \quad (4)$$

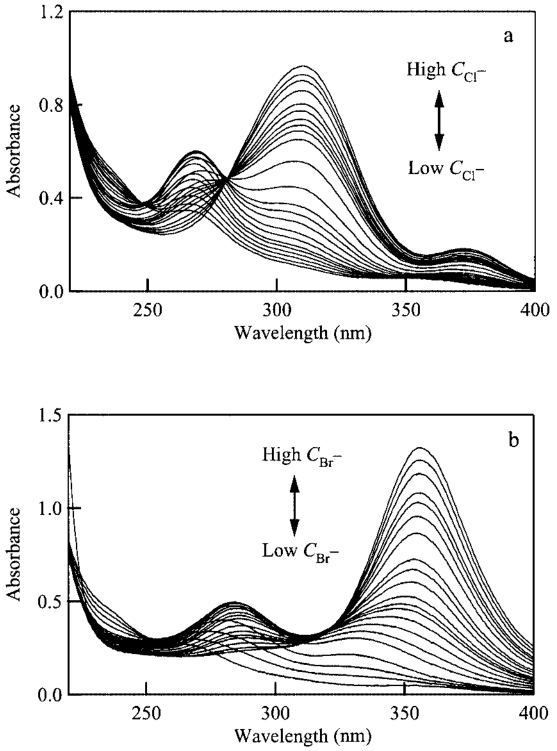

Figure 2. The UV/Vis spectra of the HH pivalamidato-bridged dimer in acidic aqueous solution with different C_{X^-} at 25 °C and $I = 2.0$ M. $[H^+] = 0.803$ M, $C_{Cl^-} = 0-1.7 \times 10^{-2}$ M (a); $C_{Br^-} = 0-1.1 \times 10^{-2}$ M (b); $C_{HH} = 3.9 \times 10^{-5}$ M (a), $C_{HH} = 3.2 \times 10^{-5}$ M (b)

The K_1^X and K_2^X values were obtained by simultaneously analyzing the spectra in Figure 1 and 2.

The values of K_{h_1}, the first acid dissociation constant (deprotonation of the H_2O ligand on the $Pt(N_4)$ atom) of the diaqua complex, was also obtained for the pivalamidato-bridged dimer. The obtained values are given in Table 1. The K_1^{Cl} and K_2^{Cl} values agree reasonably with the corresponding values for the reaction of the HH α-pyrrolidonato-bridged dimer with Cl^- (Table 1).

Kinetics for the Formation of the HH α-Pyrrolidonato- and Pivalamidato-Bridged Monohalo Complexes

The formation rate of the monohalo complex (Pt_2X) is given by Equation (5) under the present experimental conditions ($C_{HH} << C_{X^-}$), in which [HH] is the concentration of the unchanged dimer.

$$d[Pt_2X]/dt = k_{obs1}[HH] \tag{5}$$

The conditional first-order rate constant k_{obs1} is linearly dependent on C_{X^-} at a given $[H^+]$ as shown in Figure 3, thus, k_{obs1} is expressed as Equation (6):

$$k_{obs1} = k_{f1} C_{HH} \tag{6}$$

It is obvious from Figure 3 that k_{f1} in Equation (6) depends on $[H^+]$. This $[H^+]$ dependency is similar to that for the HH α-pyridonato-bridged dimer system reported previously,[13] and was successfully analysed according to Equation (7), which was derived based on Scheme 1 for the previous system.

$$k_{obs1} = \frac{k_1 + \frac{k_1^{\#} K_{h1}}{[H^+]}}{1 + \frac{K_{h1}}{[H^+]}} C_{HH} \tag{7}$$

The values of k_1 and $k_1^{\#}$ were obtained by applying a nonlinear least-squares fitting to Equation (7), and are listed in Table 2, together with the related data.

Kinetics for the Formation of the HH α-Pyrrolidonato- and Pivalamidato-Bridged Dihalo Complexes

Under these conditions, $C_{HH} << C_{X^-}$, the formation rate of the dihalo complex (Pt_2X_2) is expressed as Equation (8), where [HH-X] is the concentration of the monohalo HH dimer.

$$d[Pt_2X_2]/dt = k_{obs2}[HH\text{-}X] \tag{8}$$

The rate constant of the second substitution step, k_{obs2}, depends linearly on C_{X^-} for the reactions of the α-pyrrolidonato-bridged dimer with Cl^- and the pivalamidato-bridged dimer with Cl^- and Br^-, and nonlinearly for the reaction of the α-pyrrolidonato-bridged dimer with Br^-, as shown in Figure 4.

Table 1. Equilibrium constants for the reaction of the HH amidato-bridged *cis*-diammineplatinum(III) dimer with halide ions determined spectrophotometrically at $I = 2.00$ M and 25 °C

Bridging ligand	$-\log K_{h1}$	$\log K_1^{Cl}$	$\log K_2^{Cl}$	$\log K_1^{Br}$	$\log K_2^{Br}$
α-Pyridonate[a]	1.71 ± 0.03	5.93 ± 0.02	3.71 ± 0.01	6.20 ± 0.05	4.55 ± 0.01
α-Pyrrolidonate	3.02[b]	5.61 ± 0.03 5.23[c]	3.73 ± 0.01 3.60[c]	5.48 ± 0.02	4.68 ± 0.01
Pivalamidate	2.88 ± 0.01	5.04 ± 0.04	3.21 ± 0.01	5.93 ± 0.01	3.91 ± 0.01

[a] Ref.[13] [b] Ref.[14] [c] Ref.[15]

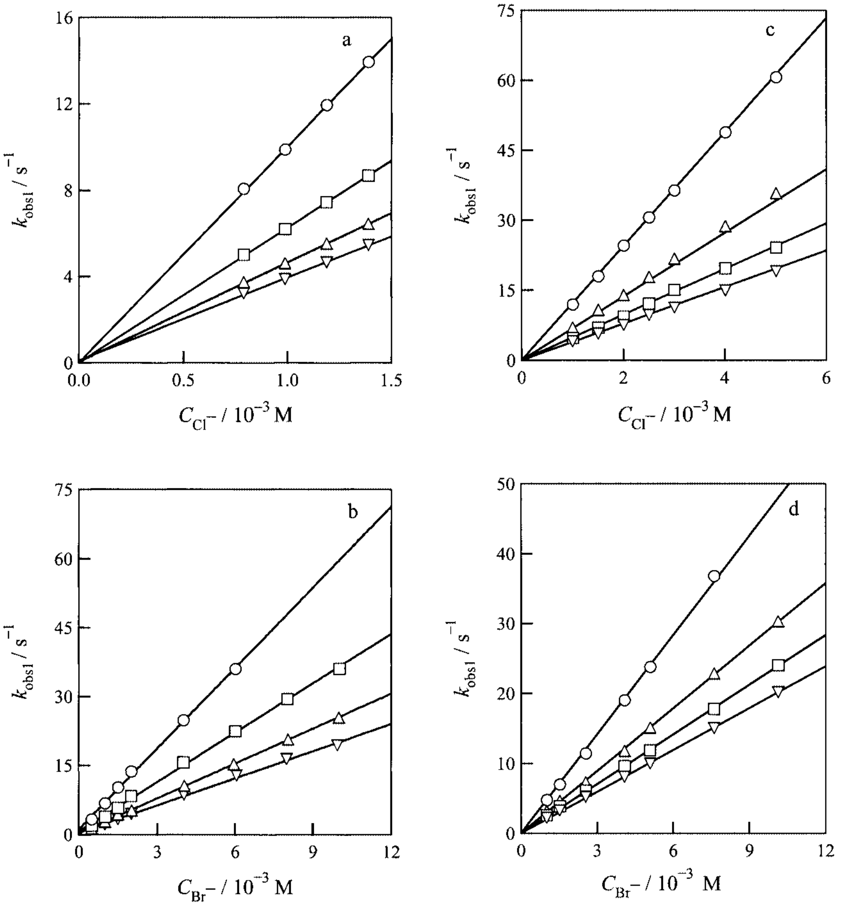

Figure 3. The dependence of k_{obs1} on C_{X^-} in acidic aqueous solution at 25 °C and $I = 2.0$ M: (a) the reaction of the HH α-pyrrolidonato-bridged dimer with chloride ion, $C_{HH} = 4.0 \times 10^{-5}$ M, $[H^+] = 0.208$ (circle), 0.401 (square), 0.602 (triangle), 0.803 M (wedge); (b) the reaction of the HH α-pyrrolidonato-bridged dimer with bromide ion, $C_{HH} = 4.0 \times 10^{-5}$ M, $[H^+] = 0.207$ (circle), 0.401 (square), 0.617 (triangle), 0.822 M (wedge); (c) for the reaction of the HH pivalamidato-bridged dimer with chloride ion, $C_{HH} = 4.0 \times 10^{-5}$ M, $[H^+] = 0.207$ (circle), 0.401 (triangle), 0.602 (square), 0.803 M (wedge); (d) for the reaction of the HH pivalamidato-bridged dimer with bromide ion, $C_{HH} = 2.0 \times 10^{-5}$ M, $[H^+] = 0.401$ (circle), 0.803 (triangle), 1.00 (square), 1.20 M (wedge)

Table 2. The rate constants for step 1 of the reactions of the HH amidato-bridged *cis*-diammnineplatinum(III) dimers with halide ions at $I = 2.00$ M and 25 °C

Ligand	Bridging ligand	Path	k [M^{-1}s^{-1}]
Cl$^-$	α-Pyridonate[a]	k_1	3.1×10^3
		$k_1^\#$	4.6×10^5
	α-Pyrrolidonate	k_1	$(1.98 \pm 0.03)\times10^3$
		$k_1^\#$	$(1.70 \pm 0.01)\times10^6$
	Pivalamidate	k_1	$(1.12 \pm 0.03)\times10^3$
		$k_1^\#$	$(1.76 \pm 0.07)\times10^6$
Br$^-$	α-Pyridonate[a]	k_1	7.2×10^3
		$k_1^\#$	2.4×10^5
	α-Pyrrolidonate	k_1	$(1.07 \pm 0.02)\times10^3$
		$k_1^\#$	$(1.00 \pm 0.16)\times10^6$
	Pivalamidate	k_1	$(1.12 \pm 0.01)\times10^3$
		$k_1^\#$	$(1.13 \pm 0.01)\times10^6$

Ref.[13]

The non-linear plot in Figure 4b is very similar to those reported previously for the reactions of HH α-pyridonato-bridged dimer with Cl$^-$ and Br$^-$, and the reaction of HT α-pyridonato-bridged dimer with Br$^-$,[12,13] i.e., k_{obs2} increases linearly with C_{Br^-} at lower C_{Br^-}, and it still increases linearly at higher C_{Br^-}, but with a different slope. This fact is explained by the mechanism in Scheme 2.

The linear plots in Figure 4d are dependent on [H$^+$], and have a close resemblance to those for the reaction of the HT α-pyridonato-bridged dimer with Cl$^-$. Therefore Scheme 3 can be proposed for the present reaction analogous to the reported α-pyridonato-bridged dimer.

On the other hand, the plots in Figure 4a and 4c have no [H$^+$] dependency and zero and non-zero intercepts, respectively. These facts correspond to simple substitutions without and with the contribution of the reverse reaction, respectively, as shown in Scheme 4.

In Scheme 2, when the steady-state approximation is applied to the monobromo dimer without an axial ligand at the opposite site, Equation (9) is obtained when the reverse reaction is negligible.

$$k_{obs2} = k_2[Br^-] + \frac{k_3 k_4[Br^-]}{k_{-3} + k_4[Br^-]} \qquad (9)$$

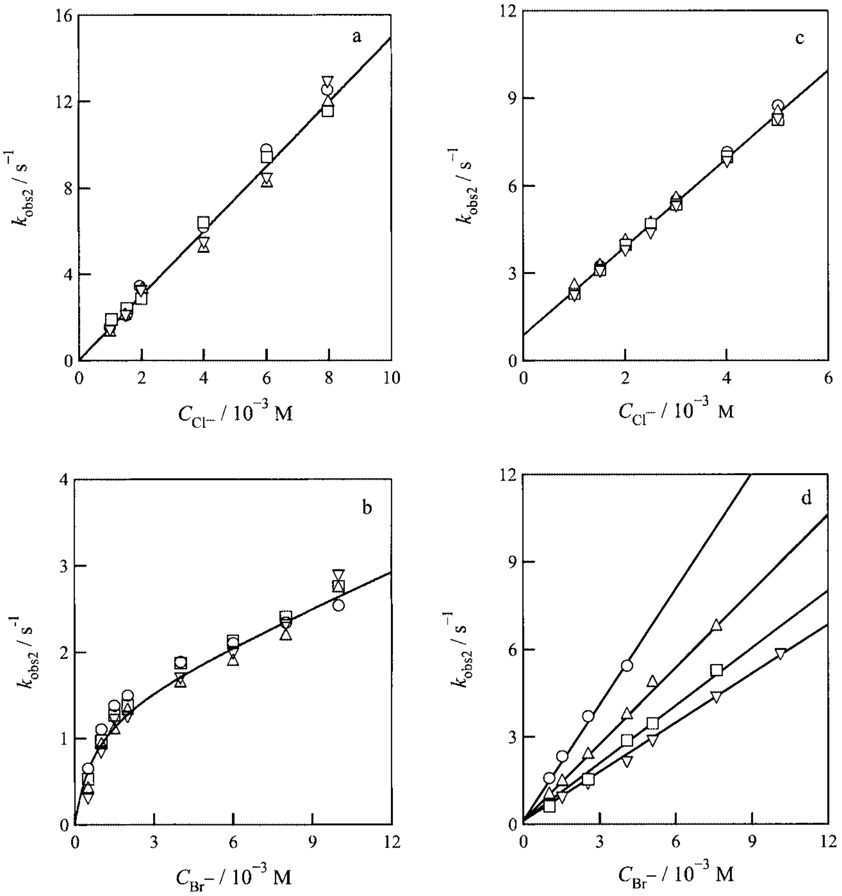

Figure 4. The dependence of k_{obs2} on C_{X^-} in acidic aqueous solution at 25 °C and $I = 2.0$ M: (a) the reaction of the HH α-pyrrolidonato-bridged dimer with chloride ion, $C_{HH} = 1.0 \times 10^{-4}$ M, $[H^+] = 0.207$ (circle), 0.401 (square), 0.617(triangle), 0.822 M (wedge); (b) the reaction of the HH α-pyrrolidonato-bridged dimer with bromide ion, $C_{HH} = 4.0 \times 10^{-5}$ M, $[H^+] = 0.207$ (circle), 0.401 (square), 0.617(triangle), 0.822 M (wedge); (c) for the reaction of the HH pivalamidato-bridged dimer with chloride ion, $C_{HH} = 4.0 \times 10^{-5}$ M, $[H^+] = 0.207$ (circle), 0.401 (triangle), 0.602 (square), 0.803 M (wedge); (d) for the reaction of the HH pivalamidato-bridged dimer with bromide ion, $C_{HH} = 2.0 \times 10^{-5}$ M, $[H^+] = 0.401$ (circle), 0.803 (triangle), 1.00 (square), 1.20 M (wedge)

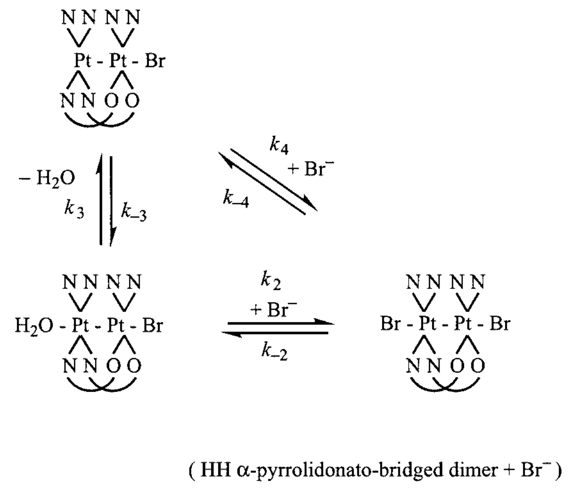

Scheme 2. (HH α-pyrrolidonato-bridged dimer + Br$^-$)

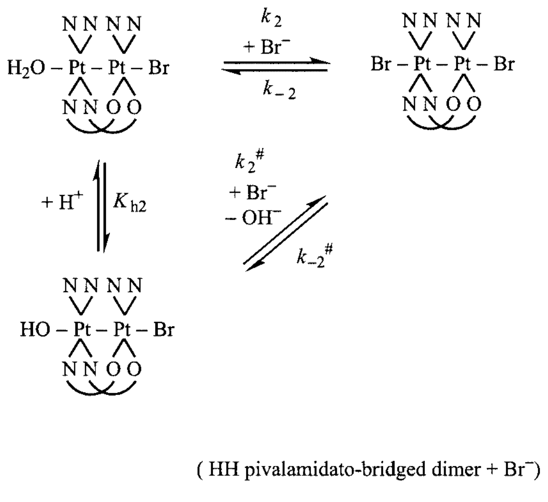

Scheme 3. (HH pivalamidato-bridged dimer + Br$^-$)

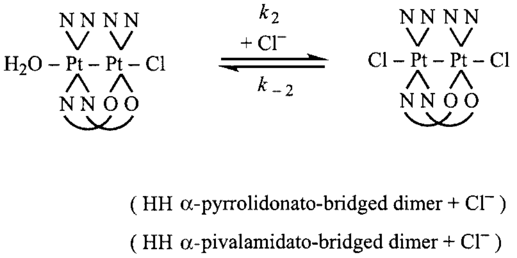

Scheme 4. (HH α-pyrrolidonato-bridged dimer + $\mathrm{Cl}^{-)}$ (HH pivalamidato-bridged dimer + Br^-)

For Schemes 3 and 4, k_{obs2} is represented by Equation (10) and (11), respectively, in which k_{-2} in Equation (11) should be omitted for the reaction of the HH α-pyrrolidonato-bridged dimer with Cl^-.

$$k_{obs2} = \frac{k_2 + \frac{k_2^{\#} K_{h2}}{[\mathrm{H}^+]}}{1 + \frac{K_{h2}}{[\mathrm{H}^+]}} C_{\mathrm{Br}^-} \tag{10}$$

$$k_{obs2} = k_2 C_{\mathrm{Cl}^-} + k_{-2} \tag{11}$$

The determined rate constants in Equation (9)−(11) are tabulated in Table 3.

Table 3. The rate constants for step 2 of the reactions of the HH amidato-bridged *cis*-diammnineplatinum(III) dimer with halide ions at I = 2.00 M and 25 °C

Ligand	Bridging ligand	Path	k [M^{-1}s^{-1}]
Cl^-	α-Pyridonate[a]	k_2	$(5.50 \pm 0.10)\times10^2$
		k_3 [b]	3.1 ± 0.3
		k_{-3}/k_4 [c]	$(3.7 \pm 0.5)\times10^{-3}$
	α-Pyrrolidonate	k_2	$(1.52 \pm 0.01)\times10^3$
	Pivalamidate	k_2	$(1.51 \pm 0.01)\times10^3$
		k_{-2} [b]	$(8.66 \pm 0.24)\times10^{-1}$
Br^-	α-Pyridonate[a]	k_2	$(4.50 \pm 0.36)\times10^2$
		k_3	4.4 ± 0.8
		k_{-3}/k_4 [c]	$(3.7 \pm 0.8)\times10^{-3}$
	α-Pyrrolidonate	k_2	$(1.36 \pm 0.07)\times10^2$
		k_3	1.39 ± 0.07
		k_{-3}/k_4 [c]	$(7.73 \pm 0.93)\times10^{-4}$
	Pivalamidate	k_2	$(1.01 \pm 0.30)\times10^2$
		k_{-2} [b]	$(1.25 \pm 0.46)\times10^{-2}$
		$k_2^{\#}K_{h2}$ [b]	$(8.52 \pm 0.81)\times10^2$

[a] Ref.[13] [b] In s^{-1}. [c] In M.

Discussion

In view of Table 1, the first acid dissociation constant K_{h1} of the α-pyridonato-bridged dinuclear complex is larger than those of the α-pyrrolidonato- and the pivalamidato-bridged complexes, whose K_{h1}'s are similar. It should be noted that the difference between $\log K_1^{\mathrm{Cl}}$ and $\log K_1^{\mathrm{Br}}$ for the pivalamidato-bridged system is larger than those for the other two systems, and $\log K_1^{\mathrm{Cl}}$ and $\log K_2^{\mathrm{X}}$ for the pivalamidato-bridged system are significantly smaller than the corresponding values for the other two systems.

The k_1 values for the reactions of the α-pyridonato-bridged complex with both Cl^- and Br^- are somewhat larger than those for the reactions of the α-pyrrolidonato- and pivalamidato-bridged complexes with the corresponding halide ions, whereas this relation is reversed for the $k_1^{\#}$ values, as shown in Table 2. As mentioned above, in the HH dimer the deprotonation occurs at the H_2O of the $\mathrm{Pt(N_4)}$ [$\mathrm{H_2O\text{-}Pt(N_2O_2)\text{-}Pt(N_4)\text{-}OH_2} \rightarrow \mathrm{H_2O\text{-}Pt(N_2O_2)\text{-}Pt(N_4)\text{-}OH} + \mathrm{H}^+$], whereas the first ligand substitution takes place at the opposite $\mathrm{Pt(N_2O_2)}$ atom [$\mathrm{H_2O\text{-}Pt(N_2O_2)\text{-}Pt(N_4)\text{-}OH_2} + \mathrm{X}^- \rightarrow \mathrm{X\text{-}Pt(N_2O_2)\text{-}Pt(N_4)\text{-}OH_2} + \mathrm{H_2O}$]; the second ligand substitution at $\mathrm{Pt(N_4)}$ is strongly influenced by the first ligated ligand on the $\mathrm{Pt(N_2O_2)}$. So, the k_1 and $k_1^{\#}$ values may reflect that the $\mathrm{H_2O\text{-}Pt(N_2O_2)}$ bond in the α-pyridonato-bridged diaqua complex is weaker than those in the α-pyrrolidonato- and pivalamidato-bridged complexes, since the $\mathrm{H_2O\text{-}Pt(N_4)}$ bond in the former complex, which has a larger K_{h1}, is stronger than those in the latter complexes which have smaller K_{h1}, and that once the diaqua complexes are deprotonated, the $\mathrm{H_2O\text{-}Pt(N_2O_2)}$ bonds in the aquahydroxo complexes become weaker for these complexes, since the opposite $\mathrm{HO\text{-}Pt(N_4)}$ bonds become stronger in the deprotonated complexes. In the dinuclear complex [$\mathrm{X_2\text{-}Pt(N_4)\text{-}Pt(N_2O_2)\text{-}X_1}$] the axial bond length [$\mathrm{X_1\text{-}Pt(N_2O_2)}$, $\mathrm{X_2\text{-}Pt(N_4)}$, and Pt-Pt] depends on both X_1 and X_2.[13] On the basis of the findings mentioned above, it follows that the bond length (and the extent of the charge localization) also changes depending on the bridging ligand.

The rate constants for step 2 are summarized in Table 3. The rate constants k_2 for the direct substitution of the monohalo complexes with halide ion (see Schemes 2−4) show that the α-pyridonato-bridged monochloro complex is less reactive than the α-pyrrolidonato- and pivalamidato-bridged monochloro complexes, whereas the α-pyridonato-bridged monobromo complex is more reactive than the other monobromo complexes. Thus, the substitution reactivity of the axial sites of the amidato-bridged dinuclear complex is considerably influenced by the bridging ligand.

The formation constant K_2^{X} (= k_2/k_{-2}) for the pivalamidato-bridged dihalo complex, derived from the rate constants (k_2 and k_{-2}) in Table 3, is in excellent agreement with K_2^{X} in Table 1 obtained by spectrophotometry [$\log K_2^{\mathrm{Cl}} = \log(k_2/k_{-2}) = 3.24$; $\log K_2^{\mathrm{Br}} = 3.91$], which supports the present kinetic analysis.

The reaction mechanism for step 1 is described in Scheme 1, in which there are two reaction pathways in all the systems under the present conditions: one is the substitution of H_2O at the $\mathrm{Pt(N_2O_2)}$ center in the diaqua complex, and the other is also a substitution of H_2O but at the $\mathrm{Pt(N_2O_2)}$ center in the aquahydroxo complex. The reaction mechanisms for step 2 are shown in Schemes 2−4. There are three possible pathways for step 2, depending on the axial ligand (X_1) at the $\mathrm{Pt(N_2O_2)}$ center, as discussed previously:[12,13] one is the direct substitution path (k_2), the second is the path (k_3) via dissociation of the water molecule ligated to the Pt(N_4), and the third is the unusual path ($k_2^{\#}$) of the OH^- replacement at the Pt(N_4). This last path is impossible in mononuclear metal complexes, but can occur in the present complexes, probably due to the contribution of the electron localization of the form HO-Pt^{II}-Pt^{IV}-X_1. When X_1 on the Pt(N_2O_2) is less electron donating, the reaction tends to proceed through the k_2 and $k_2^{\#}$ paths,

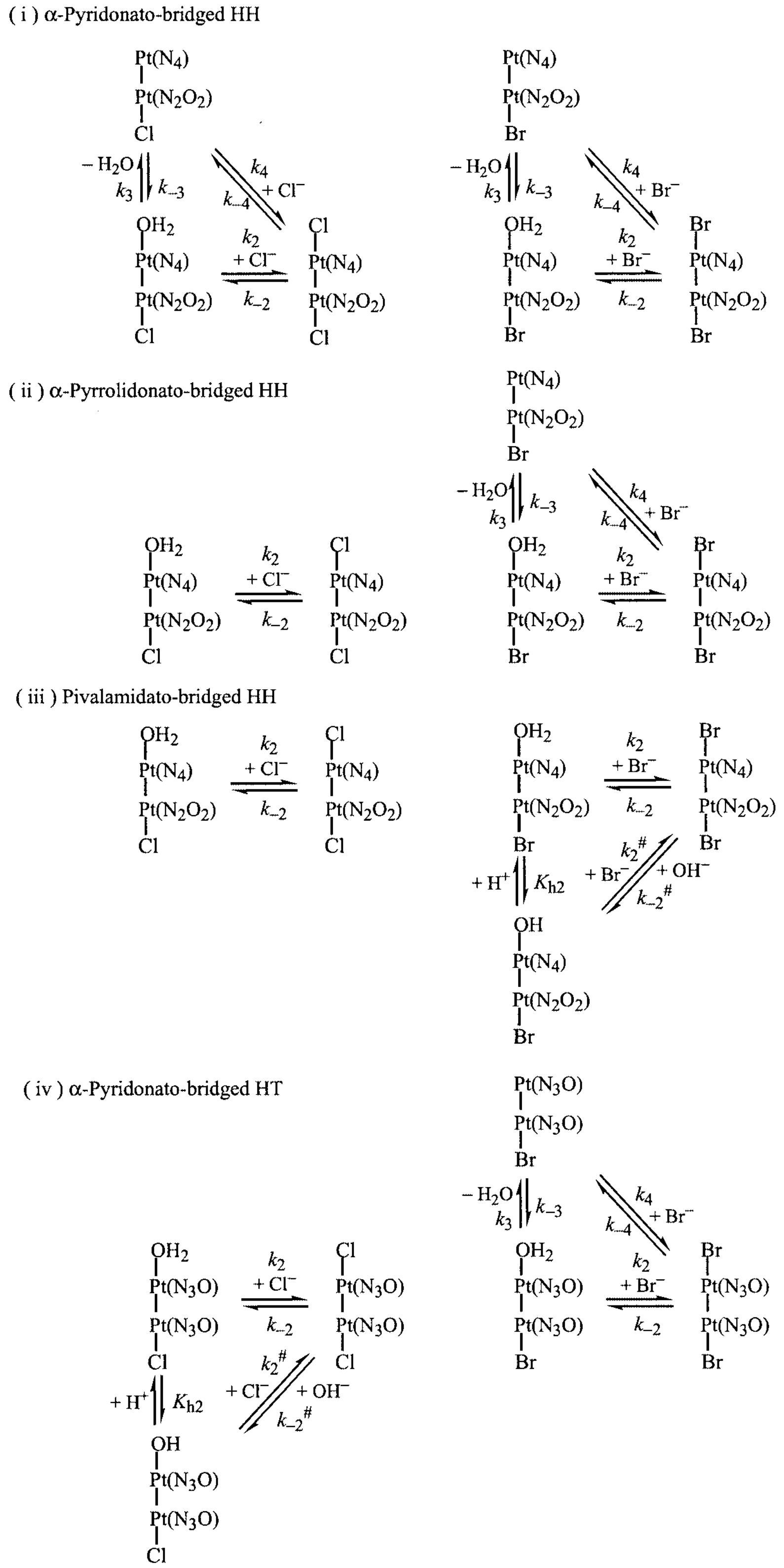

Scheme 5. Reaction pathways of the second step for the reactions of the amidato-bridged Pt^{III} dinuclear complexes with halides

whereas when X_1 is more electron donating, the k_2 and k_3 paths are preferred. The reaction schemes of step 2 for the reactions of the α-pyrrolidonato- and pivalamidato-bridged complexes are summarized in Scheme 5, together with those for the HH and HT α-pyridonato-bridged dinuclear complexes.[12,13]

The mechanistic difference in the α-pyridonato-bridged HH and HT dinuclear complexes was interpreted as follows: the difference in the HT α-pyridonato-bridged complex + Cl^- and the HT complex + Br^- systems can be reasonably explained by the relative electron donor ability of Cl^- and Br^-. Because the more electron donating Br^- facilitates dissociation of the axial aqua ligand from the opposite Pt atom, the coordinatively unsaturated intermediate is involved in the mechanism [Scheme 5 (iv)]. The charge localization through the Pt−Pt bond would be more pronounced in the HH aquahalo dimer than in the HT aquahalo dimer since the two Pt atoms are not equivalent in the HH diaqua dimer, i.e., the HH aquahalo dimer has greater $Pt^{II}(N_4)$-$Pt^{IV}(N_2O_2)$-X_1 character than the HT aquahalo dimer, and this shifts the mechanism of (iv) to the dissociative mechanism of (i) in Scheme 5. According to these explanations, the extent of charge localization in the α-pyrrolidonato- and pivalamidato-bridged monochloro complexes having only the k_2 path would be intermediate between the HH and HT α-pyridonato-bridged dimers. In the α-pyrrolidonato-bridged monohalo dimer, the charge localization of the monobromo dimer would be more pronounced than that of the monochloro dimer, whereas the opposite tendency is observed for the pivalamidato-bridged monohalo complexes. Therefore, both the bridging ligand and the axial ligand X_1 affect the mechanism. From the viewpoint of the bridging ligand, the order of the electron localization enhancement in the HH monochloro complexes is α-pyridonato-bridged complex > α-pyrrolidonato-bridged complex ≈ pivalamidato-bridged complex, and in the HH monobromo complexes, α-pyridonato-bridged complex ≈ α-pyrrolidonato-bridged complex > pivalamidato-bridged complex. Thus, in the HH amidato-bridged Pt^{III} dinuclear complexes, the effect of X_1 on the substitution reactivity of X_2 is not necessarily as expected from the *trans* effect of the axial ligand X_1, if the bridging ligand is varied.

Conclusion

In α-pyrrolidonato- and pivalamidato-bridged Pt^{III} dinuclear complexes, the first deprotonation occurs from the water molecule on the $Pt(N_4)$ center and the first nucleophilic substitution with X^- ($X^- = Cl^-$ and Br^-) occurs at the $Pt(N_2O_2)$ center. The formation of the HH monohalo complex (step 1) proceeds through two parallel paths: a simple substitution path (k_1) and a path ($k_1^{\#}$) accelerated by the trans-coordinated OH^-. The formation of the HH dihalo complex from the aquahalo complex (step 2) proceeds through only a simple substitution path (k_2) for the reactions of the α-pyrrolidonato- and pivalamidato-bridged complexes with Cl^-, and the mechanism is different from the reactions of the HH and HT α-pyridonato-bridged dimers with Cl^-. Step 2 proceeds through k_2 and a path with dissociation of a water molecule (k_3) for the reaction of the α-pyrrolidonato-bridged dimer with Br^-, and k_2 and a path with OH^- replacement by Br^- at the $Pt(N_4)$ center ($k_2^{\#}$) for the reaction of the pivalamidato-bridged dimer with Br^-. The substitution behavior in step 2 for the pivalamidato-bridged dimer system is quite different from that of the α-pyrrolidonato-bridged dimer and the HH and HT α-pyridonato-bridged dimer systems.

Experimental Section

General Remarks. Reagents: *cis*-$[PtCl_2(NH_3)_2]$ was prepared from $K_2[PtCl_4]$ (Tanaka Kikinzoku Kogyo K.K., Tokyo) according to Dhara's method.[16] Reagent grade α-pyrrolidone (Kanto Chemical Co. Inc., Tokyo) was purified once by vacuum distillation. Pivalamide (98%, Aldrich) was recrystallized twice from water. Sodium chloride (99.99%, Kanto), sodium bromide (99.99%, Aldrich), and perchloric acid (60% UGR for trace analysis, Kanto) were used without further purification. Sodium perchlorate was prepared and purified according to the literature procedure.[17] Head-to-head $[(H_2O)Pt(NH_3)_2(\mu\text{-}C_4H_6NO)_2Pt(NH_3)_2(H_2O)](NO_3)_4\cdot 2H_2O$ (HH α-Pyrrolidonato-bridged dimer) and Head-to-head $[(H_2O)Pt(NH_3)_2(\mu\text{-}C_5H_{10}NO)_2Pt(NH_3)_2(H_2O)](NO_3)_4\cdot 2H_2O$ (HH Pivalamidato-bridged dimer) were prepared according to the literature procedures.[18,19]

Measurements: Ionic strength was maintained at 2.00 м with perchloric acid and sodium perchlorate. All the sample solutions were prepared in doubly distilled water just before measurement. Spectrophotometric measurements were performed with rapid-scan/stopped-flow spectrophotometers USP-500 (Unisoku Scientific Instruments, Osaka), RSP601S (Unisoku), and SF-61DX2 (Hi-Tech Scientific, Wiltshire) and spectrophotometers UV-160A (Shimadzu, Kyoto), UV-2200 (Shimadzu), and UV-2400 (Shimadzu). Rate constants were measured by monitoring the absorbance change at 282 nm for the reaction of the HH α-pyrrolidonato-bridged dimer with Cl^- (as NaCl) and at 358 nm for the reaction with Br^- (as NaBr) for k_{obs1}, and at 268 nm for the reaction of the HH pivalamidato-bridged dimer with Cl^-, at 312 nm for the reaction of the HH dimer with Br^- for k_{obs2}, as a function of time after mixing the solutions of the dimer and sodium halide. The formation constants (K_1^X and K_2^X) of the HH monohalo and the dihalo α-pyrrolidonato- and pivalamidato-bridged dimers were determined spectrophotometrically under the following conditions. (a) For the α-pyrrolidonato-bridged dimer: $C_{HH} = 9.6 \times 10^{-4}$ м, $[H^+] = 1.27$ м, $C_{Cl^-} = 0-4.1 \times 10^{-3}$ м for K_1^{Cl} and K_2^{Cl}; $C_{HH} = 3.92 \times 10^{-5}$ м, $[H^+] = 0.401$ м, $C_{Br^-} = 0-2.11 \times 10^{-3}$ м for K_1^{Br} and K_2^{Br}; (b) for the pivalamidato-bridged dimer: $C_{HH} = 3.86 \times 10^{-5}$ м, $[H^+] = 0.803$ м, $C_{Cl^-} = 0-1.7 \times 10^{-2}$ м for K_1^{Cl} and K_2^{Cl}; $C_{HH} = 3.2 \times 10^{-5}$ м, $[H^+] = 0.8037$ м, $C_{Br^-} = 0-1.1 \times 10^{-2}$ м for K_1^{Br} and K_2^{Br}. The acid dissociation constant (K_{h1}) of the HH pivalamidato-bridged dimer was determined spectrophotometrically as described previously[12] under the conditions: $C_{HH} = 1.14 \times 10^{-4}$ м, $[H^+] = 6.69 \times 10^{-5} - 0.115$ м. All the formation and acid dissociation constants were determined with the SPECFIT program.[20] The rate constants k_{obs1} and k_{obs2} for the consecutive reaction [reactions (3) and (4)] were determined simultaneously according to the equation: $A_t = A_e + \alpha\exp(-k_{obs1}t) + \beta\exp(-k_{obs2}t)$, in which A_t and A_e are the absorbances at time t and ∞, respectively, and α and β are composite parameters.[21]

Acknowledgments

Financial Support from the 21COE "Practical Nano-Chemistry" from MEXT, Japan is gratefully acknowledged.

---

[1] R. El-Mehdawi, S. A. Bryan, D. M. Roundhill, *J. Am. Chem. Soc.* **1985**, *107*, 6282−6286 and references cited therein.

[2] S. Bryan, M. K. Dickson, D. M. Roundhill, *Inorg. Chem.* **1987**, *26*, 3878−3886 and references cited therein.

[3] R. Faggiani, B. Lippert, C. J. L. Lock, R. A. Speranzini, *J. Am. Chem. Soc.* **1981**, *103*, 1111−1120.

[4] L. S. Hollis, S. J. Lippard, *Inorg. Chem.* **1983**, *22*, 2605−2614.

[5] L. S. Hollis, M. M. Roberts, S. J. Lippard, *Inorg. Chem.* **1983**, *22*, 3637−3644.

[6] T. V. O′Halloran, M. M. Roberts, S. J. Lippard, *Inorg. Chem.* **1986**, *25*, 957−964.

[7] B. Lippert, H. Schoellhorn, U. Thewalt, *Inorg. Chem.* **1986**, *25*, 407−408.

[8] H. Schoellhorn, P. Eisenmann, U. Thewalt, B. Lippert, *Inorg. Chem.* **1986**, *25*, 3384−3391.

[9] B. Lippert, H. Schoellhorn, U. Thewalt, *J. Am. Chem. Soc.* **1986**, *108*, 525−526.

[10] [10a] T. Abe, H. Moriyama, K. Matsumoto, *Chem. Lett.* **1989**, 1857−1860. [10b] T. Abe, H. Moriyama, K. Matsumoto, *Inorg. Chem.* **1991**, *30*, 4198−4204.

[11] K. Matsumoto, K. Sakai, *Adv. Inorg. Chem.* **2000**, *49*, 375−427.

[12] N. Saeki, Y. Hirano, Y. Sasamoto, I. Sato, T. Toshida, S. Ito, N. Nakamura, K. Ishihara, K. Matsumoto, *Eur. J. Inorg. Chem.* **2001**, 2081−2088.

[13] N. Saeki, Y. Hirano, Y. Sasamoto, I. Sato, T. Toshida, S. Ito, N. Nakamura, K. Ishihara, K. Matsumoto, *Bull. Chem. Soc. Jpn.* **2001**, *74*, 861−868.

[14] K. Sakai, T. Tsubomura, K. Matsumoto, *Inorg. Chim. Acta* **1995**, *234*, 157−161.

[15] K. Sakai, Y. Tsuchiya, T. Tsubomura, *Technol. Rep. Seikei Univ.* **1992**, *54*, 77−XXXX.

[16] S. C. Dhara, *Indian J. Chem.* **1970**, *8*, 193−194.

[17] S. Funahashi, K. Haraguchi, M. Tanaka, *Inorg. Chem.* **1977**, *16*, 1349−1353.

[18] [18a] K. Sakai, K. matsumoto, *J. Am. Chem. Soc.* **1989**, *111*, 3074−3075. [18b] K. Sakai, K. Matsumoto, *J. Mol. Catal.* **1991**, *67*, 7−18.

[19] K. Matsumoto, Y. Nagai, J. Matsunami, K. Mizuno, T. Abe, R. Somazawa, J. Kinoshita, H. Shimura, *J. Am. Chem. Soc.* **1998**, *120*, 2900−2907.

[20] SPECFIT Global Analysis System by Robert A. Binstead, Bernhard Jung, Andreas D. Zuberbuhler.

[21] R. G. Wilkins, *Kinetics and Mechanism of Reactions of Transition Metal Complexes*, 2nd ed., VCH, **1991**.

Received October 7, 2002